"This is the peer reviewed version of the following article: "Geometrical scaling of the developing eye and photoreceptors and a possible relation to emmetropization and myopia" by B. Vohnsen, Vision Research, Volume 189, Pages 46-53, December 2021, which has been published in final form at https://doi.org/10.1016/j.visres.2021.09.002."

Geometrical scaling of the developing eye and photoreceptors and a possible relation to emmetropization and myopia

Brian Vohnsen*

Advanced Optical Imaging Group, School of Physics, University College Dublin, Ireland

*Corresponding author: brian.vohnsen@ucd.ie

Highlights

- The angular wave spectrum triggering vision is mainly set by the pupil size
- Photoreceptor outer-segment length is closely linked to pupil size
- Cones and rods adapt during school years when myopia onset may occur
- A photopic small pupil can prohibit leakage and crosstalk between outer segments

Abstract

In this study the role of vergence in relation to age-dependent scaling of eye and photoreceptor parameters is studied. The underlying hypothesis is that the size and packing of outer segments is matched to the pupil size outdoors in photopic conditions. Vergence is analysed in relation to the angular spectrum of waves being incident using age-dependent data from the literature for the actual geometry and density of photoreceptor cones and rods. This approach is used to derive simple relations for the angular confinement of light along outer segments. Only with a small photopic pupil can leakage and crosstalk for both central and peripheral photoreceptors be entirely ruled out due to the finite length of the outer segments. A limiting 3 mm pupil size is found for children in the school age. Larger pupils will increase the likelihood of leakage and crosstalk that may therefore impact on emmetropization. This study has introduced a new paradigm in myopia research by considering vergence across the 3-D retina as being matched to the angular spectrum of waves being incident from the eye pupil. Emmetropization suggests a delicate balance between photoreceptor outer segment length and density in relation to pupil size. Only when balanced will leakage and crosstalk between adjacent outer segments be effectively suppressed thereby ensuring the highest possible

light capture efficiency by visual pigments in the outer segments whether an image is formed on the retina or not.

Keywords

Angular spectrum, Crosstalk, Emmetropization, Leakage, Myopia, Photoreceptors, Vergence

1. Introduction

Myopia is globally on the rise and expected to affect up to 50% of the world population by 2050 [1]. Already in parts of Asia more than 90% of the population is myopic [2]. Approximately 20% have high myopia (beyond -6 dioptres) and are at increased risk of retinal complications including detachment, macular degeneration, glaucoma, and blindness. Thus, a range of studies have been undertaken to understand what causes the onset of myopia, its progression, and to identify new ways that can limit excessive eye growth. In humans, the common consensus is that genetic factors can cause myopia as well as extensive near work and limited time outdoors. In parallel, animal research is being conducted to understand how ocular growth rates can be altered in the developing eye. Clearly, the understanding of myopia is challenged by a multitude of factors that individually or in combination may all play a role.

In this study, the emphasis is on the optical difference between outdoors and indoors and the related change in vergence across the photoreceptor outer-segment layer of the retina. The pupil limits the angular spectrum of waves that can propagate through the eye and retina and this angular spectrum is largely preserved across the vitreous and retina as refractive differences across the eye are small. This optical fact has escaped detailed attention in previous studies of myopia that have focused more on the difference in viewing distances, luminance, light spectrum, dopamine levels, vitamin D, physical activity, contrast and spatial frequency contents [3-12]. The pupil size varies significantly between indoors and outdoors. Indoor illuminance in a well-lit room is typically an order of magnitude lower than outdoors. In young adults the pupil can vary from approximately 2 to 8 mm [13]. A typical outdoor pupil of approximately 2.4 mm has been reported [14]. In turn, the larger indoor pupil is typically less than 5 mm [15] and therefore smaller than predicted by merely illuminance differences.

The axial length of a new-born's eye is approximately 16.8 mm [16] but increases rapidly in the first year to approximately 20.6 mm after which the rate of growth slows [17]. New-borns are typically hyperopic by up to 3 dioptres but undergo emmetropization the following two years [18,19]. Eye size at birth influences the rate of growth in the first three years of life but not the refractive error [20]. Maintained eye growth continues during school years but slows down in late adolescence [21]. The axial length of the emmetropic adult eye is approximately 24 mm [22] but the myopic eye can grow to significantly larger axial lengths beyond 30 mm [23,24].

We have previously reported on a gradual reduction in the characteristic directionality of the psychophysical Stiles-Crawford effect of the first kind for myopic eyes with increased axial length [23]. That study found a geometrical reduction in characteristic directionality with increasing axial length where photoreceptors are further away from the entrance pupil. Photoreceptors are commonly

believed to act as biological waveguides of light due to their elongation and elevated effective refractive index [25,26]. Yet, they are far from isolated perfect optical fibres, but rather densely packed stackings of visual pigment contained within the irregular outer segment of each cellular body. Guiding of oblique light by total internal reflection increases the optical path and therefore absorption in clear contradiction with the Stiles-Crawford effect of the first kind. In consequence, the present author has shown that directional properties in vision may stem from the layered elongated structure of outer segments rather than from waveguide mechanisms [27]. This explains the appearance of the hue shift associated with the Stiles-Crawford effect of the second kind as being caused by self-screening and leakage recaptured by adjacent cone photoreceptors of another type. Leakage and crosstalk have also been studied previously in terms of the Stiles-Crawford effect of the first kind with significant leakage and recapture by adjacent cones for light incident at large pupil eccentricities [28] and for interference fringes and grating projections in the retinal plane of the related Campbell effect [28-30].

Recent numerical and experimental studies of photoreceptors have confirmed a lensing effect of the mitochondria in the ellipsoid and shown leakage of light from photoreceptors into the surrounding cellular matrix [27,31,32]. The leakage also explains why rod photoreceptors have no apparent Stiles-Crawford effect despite of being highly similar in cylindrical shape to the foveal cones [33]. Rods are surrounded by similar rods all containing identical rhodopsin. This collective grouping reduces the effective directionality, as light which is not captured by any one rod can enter similar neighbouring rods thereby flattening the directionality response. In turn, cones are clustered in three classes as S, M, and L cones according to their wavelength selectivity. Thus, isolated S cones are mostly surrounded by M and L cones whereas M and L cones are intermingled in smaller groups.

It has been proposed that the L-to-M cone ratio may differ between emmetropes and myopes [34] and recent experimental studies have found that a large L-to-M cone ratio leads to increased axial length and myopia in chickens [35]. When visually deprived with strong diffusers the eye elongates and becomes myopic in chickens, fish and mammals [36-38]. Electron microscopy has revealed cone photoreceptor changes with outer segment lamellae damage and rod elongation (possibly to increase low-light capture) in form-deprivation myopia with opaque occluders [39]. Optical coherence tomography (OCT) has shown outer segment elongation correlated with axial length in myopic eyes [40] as well as choroidal thinning [41]. Recently, we showed that the sensitivity to the sign of defocus may be broken either by a tapered shape of the outer segments or by the axial gradient in visual pigment density where light traverse new pigments before reaching the older pigments near the outer tip of the cones [42]. Photoreceptors have also shown to be adaptable to changes in illumination conditions as revealed in directional light scattering [43,44] and in light-induced optical path differences caused by a combination of elongation and dielectric changes following light absorption [45]. The anterior eye projects the light onto the retina where images are sampled in 3-D by the shape

and packing of the visual pigments in the photoreceptors, the ganglion cells and the neural pathways to the visual cortex. Thus, a detailed understanding of the light distribution across the entire retina is of relevance when examining factors that can play a role for myopia onset and progression.

The infant pupil size is typically larger than in adults [46]. At birth, cone photoreceptors are wider and shorter than in the adult eye and have lower absorption [47]. The photoreceptors are packed less densely in the first years of life where cone migration continues to take place while the foveal pit formation completes [48]. At an age of approximately 4 years the shape of the foveal pit resembles that of the adult [49,50] although the outer segment length and cone packing density is still only half as large [48,51]. The increase in foveal inner and outer segment length is logarithmic until 26.9- and 45.3-months gestational age whereas the corresponding increase in the parafoveal and perifoveal retinal layers is more gradual until 146-months gestational age [50]. In the peripheral retina, cones are shorter and highly separated with the spacing filled by rods. Myopia onset occurs typically in early school years at an age of about 6 to 10 years and progresses during teenage years [52,53]. At this age changes in the retina and photoreceptors have slowed down but are still present. The hypothesis of this study is that the age-dependent size and packing of outer segments in the developing eye are carefully balanced to the ideal outdoor pupil size in photopic conditions.

2. Method

A simplified eye model consisting of a single lens with focal length matched to the axial length (AL) as shown in Fig. (1) will be used. The model relates the angular spectrum of waves across outer segments to vergence of planar wave vectors, $\boldsymbol{k}$, provided by a given pupil size. Although this is a highly simplistic model, it gives an accurate estimate of the angular spectrum of waves being incident onto the retina in the real eye.

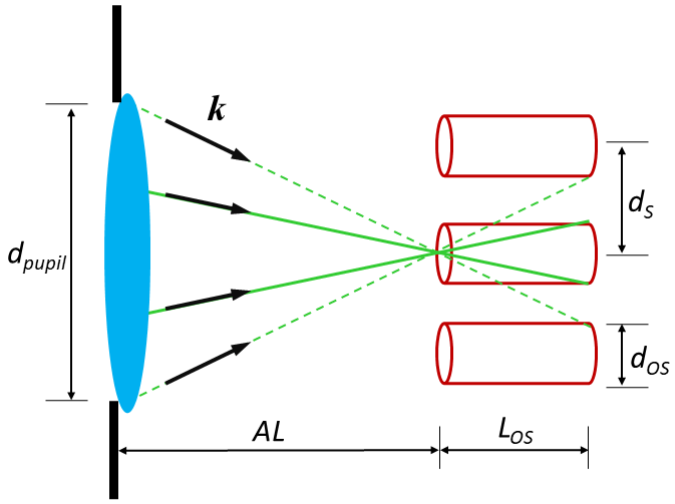

Figure 1: Simplified eye model (not-to-scale) to match vergence from the pupil to the photoreceptor outer segments of rods or cones where absorption triggers vision. The solid green lines represent

angles from a small pupil where planar wave components cannot leak from the cylindrical outer segments. In turn, the dashed green lines show planar wave components from a larger pupil that are at the limit of entering neighbouring outer segments causing crosstalk.

Light propagation in any medium can be fully described by the angular spectrum method. This is normally done for light propagation between planar surfaces but is equally valid in a spherical geometry [54]. For a large pupil, aberrations would perturb the angular spectrum whereas for a small pupil diffraction would ultimately widen the angular spectrum contained within the Airy disk. However, the diffractive spread is small (<5%) with a natural pupil of 2 mm or more [55]. Aberrations only alter the vergence of the wave vectors slightly. A large impact of aberrations in the retinal plane is due to the accumulated effect when propagated across the full AL of the eye. The angle of incidence on the retina is largely determined by the pupil entry point and only little affected by monochromatic and chromatic aberrations. A highly aberrated eye as well as chromatic aberrations will shift the rays in the retinal plane typically by tens to hundreds of microns (thereby degrading the visual acuity) whereas an offset pupil entry point is in the order of millimetres. In other words, the angle of incidence is typically altered less than 10% by aberrations. Longitudinal chromatic aberrations will shift the focus across the retina but only alter the angle of incidence by up to 2% across the visible spectrum.

The model differentiates between waves according to angle, but not whether an image is formed in the retinal plane or not. I.e, it considers angular confinement not spatial confinement of light. Even a uniform bright environment without contrast or features will be equally valid while the vergence across the photoreceptors is small. The largest absorption is ensured when light is incident close to the axis of each photoreceptor as evident by the Stiles-Crawford effect of the first kind. The visual pigments within individual outer segments act to maximize their photon catch oblivious of the light environment on adjacent photoreceptors. Considering the wave vector angles within and between each outer segment is equivalent to the use of the Rayleigh hypothesis widely used in the plane-wave analysis of deep diffraction gratings [56].

Optical vergence, photoreceptor leakage and crosstalk

The simplified eye model in Fig. 1 is shown with cylindrical outer segments (as representative of foveal cones or peripheral rods). For simplicity, the axial length used excludes the inner retina layer, inner segment and ellipsoid as these add less than 1% to the distance. The limiting lines represent wave vectors whose angular spectrum is determined by the pupil size, d_{pupil}, and thus by the vergence. I.e., they represent the most oblique wave-vector components as permitted by the pupil.

If light is to be confined within the outer segment the following condition must be satisfied:

$$d_{pupil} \leq AL \frac{d_{OS}}{L_{OS}}. \quad \text{Eq. (1)}$$

Here, d_{OS} is the (assumed cylindrical) outer segment diameter and L_{OS} is the outer segment length. Thus, geometrically each cone cross section is a scaled-down version of the eye pupil. If the pupil diameter is larger than set by Eq. (1) leakage from outer segments can occur. Yet, this would not impact vision unless light enters adjacent outer segments with a similar or identical absorption spectrum. To avoid such crosstalk, the following condition must be met:

$$d_{pupil} \leq AL \frac{2d_s - d_{OS}}{L_{OS}} \quad \text{Eq. (2)}$$

where d_S is the spacing between adjacent outer segments. For a hexagonal arrangement of photoreceptors with density, σ, the following relation can be derived [57]:

$$d_S = \frac{1.075}{\sqrt{\sigma}}. \quad \text{Eq. (3)}$$

For the cones, the density is a combination of S, M and L cones that may be expressed as $\sigma = \sigma_S + \sigma_M + \sigma_L$. The S cone density is very low and likely entirely absent at the central fovea [58] whereas the densities of M and L cones vary significantly between individuals with a typical L to M ratio of 2:1 [59,60]. In this study an S:M:L relation of 5%:30%:65% will be assumed that combined provide the spectral response of the eye [61].

The axial length of the eye (in mm) increases logarithmically with age as shown in Eq. (4) for an emmetropic eye using data from Ref. [17] (less than 90 months) and Ref. [53] (above 6 years):

$$AL_{emmetropic} = \begin{cases} 20.670 + 0.966 \times \ln(\text{age}); & \text{age} < 7.5 \text{ years} \\ 20.189 + 1.258 \times \ln(\text{age}); & 6 \text{ years} < \text{age} \leq 10.5 \text{ years} \\ 21.353 + 0.759 \times \ln(\text{age}); & \text{age} > 10.5 \text{ years} \end{cases}. \quad \text{Eq. (4)}$$

These data are from two different studies but differ only slightly in the overlapping age interval from 6 to 7.5 years. In turn, the rate of change is higher for the average myopic eye [53] as shown in Eq. (5):

$$AL_{myopic} = \begin{cases} 18.144 + 2.391 \times \ln(\text{age}); & 6 \text{ years} < \text{age} \leq 10.5 \text{ years} \\ 17.808 + 2.560 \times \ln(\text{age}); & \text{age} > 10.5 \text{ years} \end{cases}. \quad \text{Eq. (5)}$$

Plots of Eqs. (4) and (5) are shown in Fig. 2.

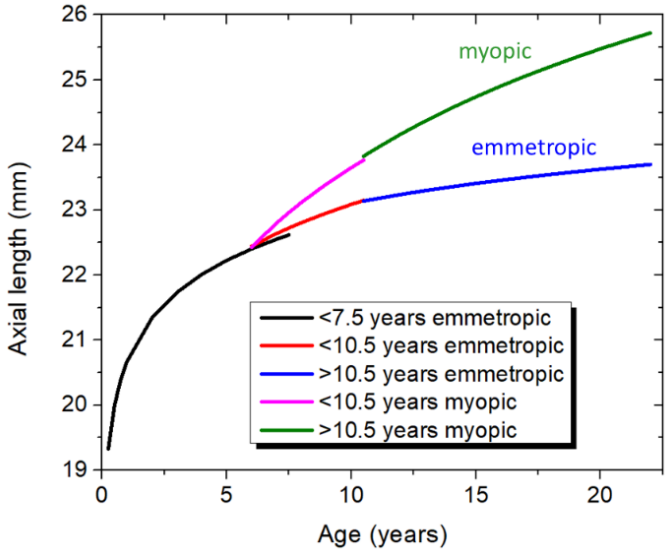

Figure 2: Axial length versus age in the developing eye based on data from the literature for emmetropes and myopes in the USA. Ref. [17] shows average data for 165 children less than 7.5 years and Ref. [53] shows average data for 247 myopes and 194 emmetropes, respectively in two age groups from 6 – 10.5 years and from 10.5 years and upwards.

There is a large variation in photoreceptor data for infants, children and adult eyes. In the new-born infant foveal cones are very wide (about 7.5 μm) and short (about 10 μm) [48]. The outer segment itself is just about 3 μm long but increases rapidly during the first year of life. In Eq. (6) the outer segment length (in μm) is given using fractional polynomial regression fitting of OCT data in Ref. [50]:

$$L_{OS}^{fovea} = -0.2384 \times (10^4/(12 \times \text{age} + 9)^2 - 2.928) + 32.36 \qquad \text{Eq. (6)}$$

for age > 0.25 years (3 post-natal months). The OCT determination of outer segment length has been done in accord with anatomy [62] although a strict match to the length of membrane invaginations is challenging and some studies report larger OS lengths. In the parafovea and perifovea cone outer segments are shorter. Parafoveal photoreceptors develop prior to the foveal cones and cone outer segments elongate in the first 5 years of life whereas rod outer segments continue to elongate until an age of approximately 13 years [63]. In adults with normal vision the outer segment length varies little [64,65]. In the parafoveal retina (1 mm eccentricity) the cone outer segment length varies with age as determined in Ref. [50]:

$$L_{OS}^{parafovea} = -0.069 \times (10^4/(12 \times \text{age} + 9)^2 - 2.536) + 13.64\,. \qquad \text{Eq. (7)}$$

A plot of Eq. (6) and Eq. (7) is shown in Fig. 3. It should be stressed that the spread in OCT-determined outer segment length with age is large with R-square values of 0.6388 (fovea) and 0.1989 (parafovea) [50]. This also agrees with large variations seen in histology studies [51,62].

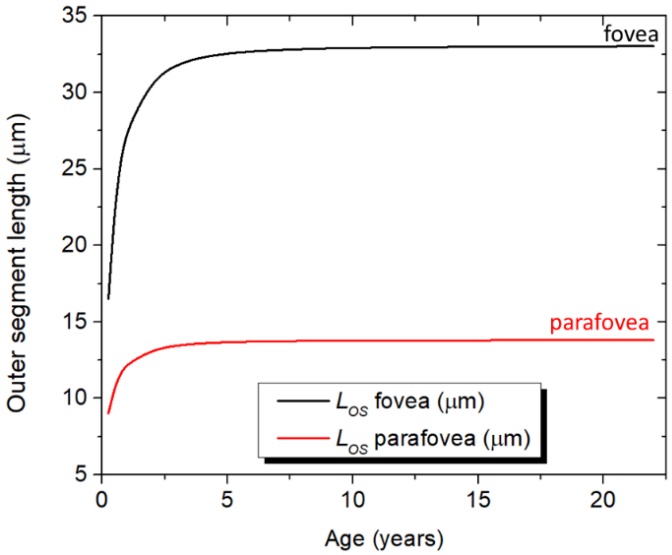

Figure 3: Cone outer segment length determined with OCT for the foveal and temporal parafoveal retina (at 1 mm eccentricity) based on data in the literature for 261 infants, children and young adults in the UK from Ref. [50].

The last parameter considered is the age-dependent peak density of cone photoreceptors. It increases rapidly in the first few years after birth until settling at adult levels. Although data is very limited, a logarithmic fit of the peak foveal cone densities (number/mm^2) from Ref. [48] using data for 5 days, 15 months and 45 months and for a 37-year adult gives a cone photoreceptor density:

$$\sigma = 96963 + 20146 \times \ln(\text{age})\,. \qquad \text{Eq. (8)}$$

A small reduction in foveal cone density for elongated eyes has been reported using scanning laser ophthalmoscopy [66] although variations impact the accuracy of data at the foveola. A plot of Eq. (8) is shown in Fig. 4. At older age (>60 years) there may be a slow decrease in peak cone density again, but that is not central for this study. The logarithmic fit in Eq. (8) was chosen for simplicity and due to the limited data available. It can be improved when more anatomical data becomes available for different age groups relevant for myopia. A tighter fit (using line segments or splines) would increase the rate of change across the school years of a child but data in the 5 to 20 years range is needed for higher accuracy. For example, a linear fit of cone density between 45 months and 37 years lowers the

absolute cone density by up to 13% at 5 years corresponding to a 7% change in d_S using Eq. (3). This impacts equally on crosstalk as specified by Eq. (2) but not on leakage as specified by Eq. (1).

In the following section the parameters summarized in Figs. (2) – (4) will be examined in relation to the angular spectrum shown in Fig. (1) and expressed by Eqs. (1) and (2).

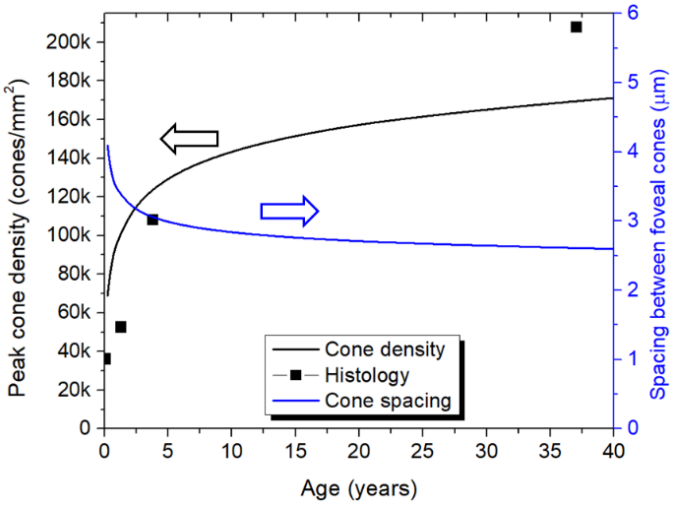

Figure 4: Foveal cone peak density as a function of age based on limited histology data points (square symbols) from the literature [48] fitted to Eq. (8) with R-squared 0.7385. The plot also shows the corresponding cone centre-to-centre spacing (assuming a hexagonal packing) using Eq. (3).

3. Results

Pupil size and photoreceptor light confinement in relation to outer-segment leakage and crosstalk

Eq. (1) allows determination of an age-dependent maximum pupil size to avoid leakage from any given outer segment as shown in Fig. (5). In turn, Eq. (2) allows determination of a maximum pupil size that will ensure no crosstalk between outer segments as shown in Fig. (6). There is some variation in reported foveal outer segment diameters, but they are mostly in the range of 1.0 to 1.5 μm. To evaluate its role, two different outer segment diameters have been included in the plots: one in the middle of the range of 1.2 μm (resembling the rods) and the other at a larger 2.0 μm which is more representative of the tapered outer segments of cones in the parafovea and peripheral retina.

Fig. (5) shows that leakage of light from foveal outer segments is essentially unavoidable across all ages. In turn, for the shorter parafoveal and peripheral outer segments leakage is prevented by a pupil size of 2 mm. The likelihood of crosstalk between foveal outer segments as shown in Fig. (6) is highly dependent on pupil size. Although the infant eye can tolerate a large pupil, at school age only a pupil size of 3 mm or less can ensure that there is no crosstalk. Any pupil size larger than that, such as a typical indoor pupil, may cause crosstalk. The fitting error in Fig. 4 has little impact on this result

as a variation in final foveal cone density from 160,000 to 170,000/mm^2 impacts on the crosstalk-free pupil diameter calculated from Eq. (2) by less than 0.1 mm.

Cone photoreceptor crosstalk is not an issue in the parafovea and beyond due to the larger spacing between shorter outer segments whereby pupil diameters up to 8 mm are acceptable. This can also be appreciated from Fig. 7 that shows the maximum pupil size to avoid crosstalk for different peripheral cone densities. Once the age-scaled cone density is lower than 40,000/mm^2 in the adult eye, corresponding to a retinal eccentricity of approximately 0.5 mm (or 2 visual degrees) the pupil size is no longer a limit.

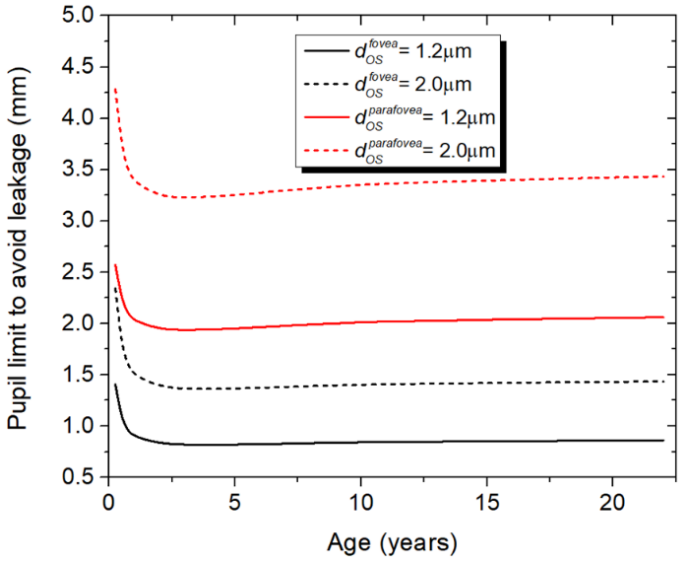

Figure 5: Maximum pupil size from Eq. (1) to avoid leakage of light from foveal (black) and parafoveal (red) outer segments using the data summarized in Figs. (3) – (5). The plots show data for an outer segment diameter of 1.2 µm (solid line) and 2.0 µm (dashed line).

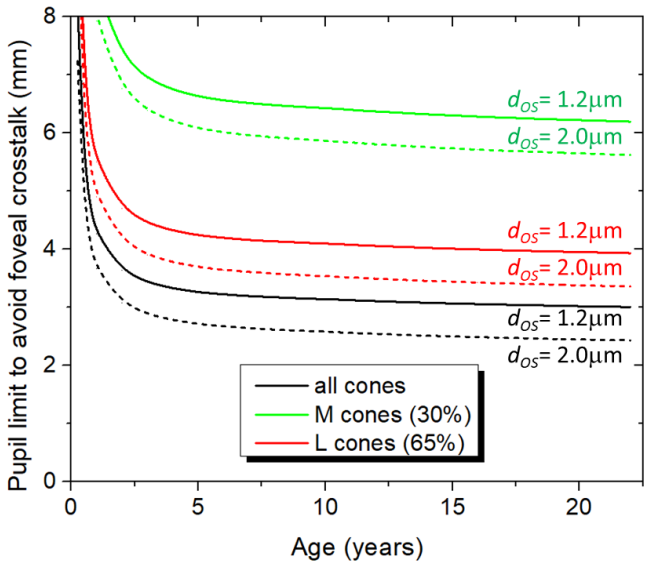

Figure 6: Maximum pupil size from Eq. (2) to avoid crosstalk between adjacent foveal outer segments using the data summarized in Figs. (2) – (4). The plots show data for an outer segment diameter of 1.2 μm (solid line) and 2.0 μm (dashed line) and including all cones, only L cones (red) and only M cones (green). Due to the low density of S cones (blue) their pupil limit is beyond the natural eye pupil at all age groups. In the parafovea and perifovea where the cone density is lower than 40,000/mm^2 crosstalk is not an issue due to the larger spacing between outer segments (see Fig. 7).

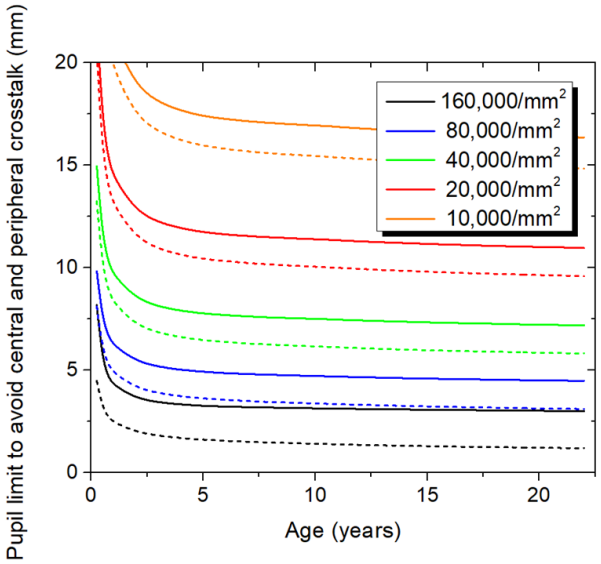

Figure 7: Maximum pupil size from Eq. (2) to avoid cone crosstalk between adjacent central and peripheral outer segments using the data summarized in Figs. (2) – (4). The plots show data for an outer segment diameter of 1.2 μm (solid line) and 2.0 μm (dashed line) for all cones. The age-dependent maximum cone density has been scaled to resemble that of the central-to-peripheral retina with adult peak cone densities of 160,000/mm^2 (black), 80,000/mm^2 (blue), 40,000/mm^2 (green), 20,000/mm^2 (red) and 10,000/mm^2 (orange).

The model in Fig. 1 allows calculation of an angular light confinement parameter, C, determined as the fraction of light within a given outer segment in relation to that in the same segment and adjacent outer segments. Whether there is crosstalk is determined by the angular vergence. The analysis can be done by calculating the volumetric overlap (intersection volume) between the light and the corresponding outer segments [33]. Without any crosstalk, C will equal unity, but once light can leak into adjacent outer segments it drops. Fig. 8 shows calculated angular confinement in the photoreceptor cones at 3 ages: 6-month infant, 4-year-old child and 14-year-old adolescent. To evaluate the impact of myopia the axial length was increased by +1 mm (approximately -3 dioptres). For example, it shows that a 14-year-old adolescent with an indoor 4 mm pupil will increase the light confinement from 0.72 to 0.88 (i.e., a 22% increase) by an AL increase of +1 mm. The increased axial length caused by myopia reduces the crosstalk and thereby raises the light confinement.

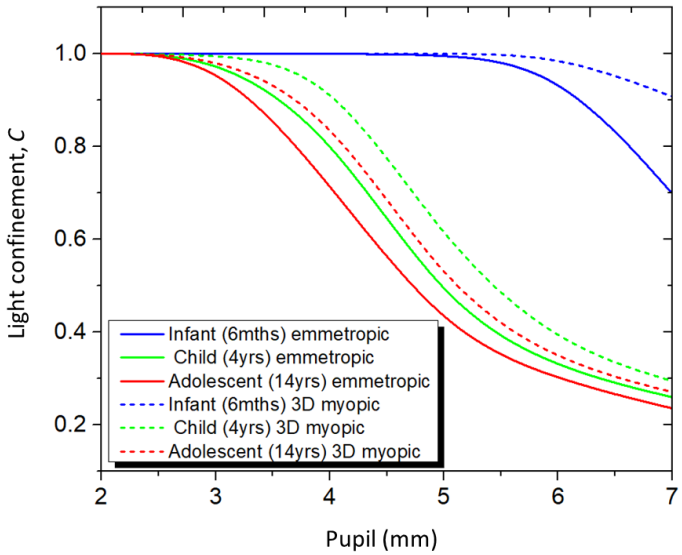

Figure 8: Calculated light confinement parameter in the effective foveal retinal image determined by the ratio of light within a given outer segment over the total light captured by the group of exposed outer segments with diameter of 1.2 μm for emmetropes (solid lines) and -3 dioptres myopes (dashed lines) obtained by +1.0 mm axial length. Parameters have been chosen for a 6-month infant (blue), a 4-year-old child (green) and a 14-year-old adolescent (red).

If an image is formed on the retina, then the capture efficiency C_I for any given photoreceptor is proportional to the volume of visual pigments (cylinder) with respect to the volume of focused light (cone) [33,42] which can be expressed as

$$C_I \cong 3\left(\frac{d_{OS}}{L_{OS}}\right)^2 \times \left(\frac{AL}{d_{pupil}}\right)^2. \qquad \text{Eq. (9)}$$

Here, the factor of 3 stems from the volume calculation, i.e., $V_{cylinder}/V_{cone}$. From Eq. (9) a doubling of pupil size leads to a 75% reduction in the light capture for any individual outer segment. When viewing an extended scene, adjacent point-spread-functions (PSF's) will raise the capture efficiency again so that it would not be perceivable, but the associated waves traverse the outer segment at different angles. Importantly, Eq. (9) shows directly that a larger d_{pupil} requires a larger AL to maintain the same capture efficiency for any outer segment, unless the outer segment itself changes diameter or length. The latter happens in childhood and early school years as described in Sec. 2.

With myopic defocus, the cone of light rays would shift its apex to the image plane in front of the retina and at the outer segment it would become a truncated cone of light [42]. The capture of the individual segment will resemble that of Eq. (9) but will quickly depend inversely on the axial shift of the focus rather than on L_{OS}. Yet, an axial shift of the focus by merely L_{OS} (approximately -0.1

dioptres) would lower the capture of the individual outer segment by up to a substantial 86% replacing the factor 3 in Eq. (9) with 3/7, light that would then become available for adjacent photoreceptors. It is important to bear in mind that Eq. (9) has been derived under simplified conditions that only consider the angular spectrum contained within the light at focus but not the spatial details of diffraction.

4. Discussion

Within the presented angular spectrum model and geometrical scaling, two different factors may impact myopia: (i) a large pupil size and therefore large angular vergence across the retina and (ii) an increase in photoreceptor densities and outer segment length coinciding with the school years of a child. Thus, it becomes increasingly likely that leakage and crosstalk will take place between adjacent outer cone segments or leakage from longer and longer rods. To limit this, either the pupil should be small, as when outdoors, or the retina should be further away from the pupil. The latter may occur in excessive indoor environments with dim light and large pupil thereby driving myopia as shown in Eq. (9). I.e., a larger pupil size is geometrically matched to a larger AL.

The model considers only the angular spectrum of waves, independent of image formation within the eye. I.e., ideally all waves travel along each photoreceptor axis to maximize light capture. Aberrations in the anterior eye will perturb the angular spectrum set by the pupil vergence, but only as a disturbance that has little impact on the angles of the waves due to the small contrast in refractive indices across the eye. Aberrations in the pupil plane correspond to intensity and phase changes of the light in the retinal plane. For monochromatic aberrations, all even-order radial Zernike terms (defocus, astigmatism, spherical aberration, etc.) have wavefront curvature at the retina whereas odd-order radial Zernike terms (coma, trefoil, etc.) are incident along the photoreceptor axes in the retinal plane and therefore less subject to leakage and crosstalk despite of the degraded PSF [55]. This implies a reduction in angular confinement of even-order Zernike terms, but not for the odd-order terms on their own. This knowledge is relevant when discussing the role of higher-order aberrations in myopia control [67]. Neural factors will also have an impact but are beyond the scope of the present study [68].

The model applies equally for the central cones as for the peripheral rods and cones. In mesoscopic vision both rods and cones contribute and thus leakage of light for large pupils affects the peripheral photoreceptors in the same manner as the central cones. The outer segment of rods is slightly longer and thinner than the cones in the periphery. The same principles as discussed for the foveal cones in Fig. 6 and Fig. 7 can be applied for the peripheral cones and for the rods. A pupil size close to 2 mm will eliminate cone and rod leakage and a pupil size below 3 mm will eliminate rod crosstalk where the rods are densest. The highest density of rods in the human retina forms a ring

approximately 20° from the foveal centre [51]. Thus, dim indoor light in mesoscopic conditions with a large pupil may impact light capture of both rods and cones in the same way as for the foveal cones.

The model introduced in this study assumes a certain plasticity in all components of the eye and retina as they adapt to the ongoing changes during childhood and adolescence. Such a process is in addition to diurnal variations that alter the eye and retinal layers at shorter time scales [69,70].

Low-concentration atropine is widely used to slow eye growth in myopia control and is known to increase the pupil size [71]. In the present model, this seems counterintuitive unless the pupil size is less than 3 mm to avoid crosstalk. A possible explanation could be a reduction in outer segment length over time to provide the same light capture efficiency. A 10% increase in pupil diameter [71] may plausibly be accompanied by an up to 10% reduction in outer segment length. To evaluate whether this happens, it would be highly desirable to study outer segment length with optical coherence tomography in children before and after completed atropine treatment.

Blue light is often being used to slow eye growth by exploring the short-wavelength refraction that brings light to a focus slightly in front of the retina [72], similar to how myopia management in peripheral vision is controlled [67]. In terms of the model introduced, this appears mostly relevant with large pupils. However, it is possible that also rods will play a role with blue light as a reduced rod density in myopes has recently been observed with scanning laser ophthalmoscopy [73].

There is some evidence that domesticated animals are more myopic than their wild counterparts. Dogs, even guide dogs, are often myopic [74]. Domesticated horses [75] and sheep are also often myopic [76]. These findings are highly impacted by genes of domesticated animals and Darwinian selection in the wild. Yet, a clear difference is also the irradiance in the animal habitats and therefore the diurnal variation in pupil size. Nocturnal animals tend to have larger pupils yet the tapetum lucidum will favour light travelling along the photoreceptor axis equivalent to a reduced angular spectrum.

Prolonged dim light during growth leads to a myopic shift both in animals [77] and humans [78]. In mesoscopic conditions there may be relevant signal pathways both in the rods and cones. Studies with chicks wearing opaque occluders have seen an initial rapid increase in rod outer segment length to nearly twice the normal length as well as widening within the first week, reducing the gap to the retinal pigment epithelium, but dimensions are nearly normalized at 4 weeks. However, the cone outer segment lengths increased by approximately 20% even after 4 weeks [39]. This seems to suggest that the photoreceptors elongate to improve light capture, but in the absence of light the mechanism settles. It is interesting to note that in the adult, where L_{OS} and d_{OS} no longer change significantly, Eq. (1) and Eq. (2) suggest that d_{pupil} is proportional to AL if leakage and crosstalk remains unchanged. This is in good correspondence to recent findings for 139 subjects aged 50 – 75 years grouped as hyperopic, emmetropic, low and moderate myopes [79]. They found that the dark-adapted pupil of moderate

myopes was approximately 7.5% larger than for the emmetropes which in terms of AL is an increase of approximately 1.8 mm.

The optical model introduced in this study may assist to gain further understanding into the complex processes of myopia onset or development. Yet, other factors are also at play both in the central and peripheral retina, including the actual mechanics involved in shaping the globe of the eye. However, it does seem to provide a plausible explanation for the benefits of time outdoors in terms of a reduced impact of oblique light rays and aberrations due to the smaller pupil. This is an optical effect that adds to the other known benefits of being outdoors. More data on photoreceptor densities, diameter, length and shape in both the central and peripheral retina for school-aged children is still vital to validate or disprove the model. The model may be tested via improved histology and OCT photoreceptor data for the myopia-critical age range, small external pupils or corneal aperture inlays in conjunction with bright light may be used to simulate outdoor conditions in animal studies, and differences between hyperopes, emmetropes and myopes in terms of photoreceptor densities, outer segment length and pupil size may provide valuable inputs.

Conclusion

In this study, an angular spectrum model for light propagation from the eye pupil and across the outer segments of the photoreceptors has been proposed using age-dependent eye and photoreceptor data from the literature. The results show that outer segment length, both at the fovea and in the peripheral retina, is well matched to a small pupil size such as when outdoors in phototropic conditions. The importance of time outdoors to prevent myopia onset appears therefore intricately linked to the optics of the photoreceptors since only with a pupil smaller than 3 mm can crosstalk between adjacent photoreceptors be ruled out, but experiments are still needed to verify the role of a small pupil in the context of preventing myopia in bright light. For larger pupils, light will propagate at larger angles through the retina whereby the likelihood of leakage and crosstalk increases. Thus, the optics of the anterior eye and pupil in the healthy emmetropic eye appear to interact with the optics of the retina as a delicately balanced system [80].

Disclosure

The author reports no conflicts of interest and have no proprietary interest in any of the materials mentioned in this article.

Acknowledgements

This research has been realized with financial support provided by the H2020 ITN MyFUN grant agreement No. 675137.

References

1. B. A. Holden, T. R. Fricke, D. A. Wilson, M. Jong, K. S. Naidoo, P. Sankaridurg, T. Y. Wong, T. J. Naduvilath, and S. Resnikoff, “Global prevalence of myopia and high myopia and temporal trends from 2000 through 2050,” Ophthalmology 123(5), 1036-1042 (2016).
2. E. Dolgin, “The myopia boom,” Nature 519, 276-278 (2015).
3. L. A. Jones-Jordan, L. T. Sinnott, S. A. Cotter, R. N. Kleinstein, R. E. Manny, D. O. Mutti, D. Twelker, and K. Zadnik, “Time outdoors, visual acuity, and myopia progression in juvenile-onset myopes,” Invest. Ophthalmol. Vis. Sci. 53, 7169-7175 (2012).
4. J. C. Sherwin, M. H. Reader, R. H. Keogh, A. P. Khawaja, D. A. Mackey, and P. J. Foster, “The association between time spent outdoors and myopia in children and adolescents” Ophthalmology 119(10) 2141-2151 (2012).
5. E. G. Landis, H. N. Park, M. Chrenek, L. He, C. Sidhu, R. Chakraborty, R. Strickland, P. M. Iuvone, and M. T. Pardue, “Ambient light regulates retinal dopamine signaling and myopia susceptibiblity,” Inv. Ophthalmol. Vis. Sci. 62(1):28 (2021).
6. A. N. French, R. S. Ashby, I. G. Morgan and K. A Rose, “Time outdoors and the prevention of myopia,” Exp. Eye Res. 114, 58-68 (2013).
7. X. Zhou, M. T. Pardue, P. M. Iuvone, and J. Qu, “Dopamine signaling and myopia development: what are the key challenges," Prog. Retin. Eye Res. 61, 60-71 (2017).
8. G. Lingham, D. A. Mackey, R. Lucas, and S. Yazar, “How does spending time outdoors protect against myopia? A review.” Br. J. Ophthalmol. 104(5), 593-599 (2020).
9. L. Wen, Y. Cao, Q. Cheng, X. Li, L. Pan, L. Li, H. Zhu, W. Lan, and Z. Yang, “Objectively measured near work, outdoor exposure and myopia in children,” Br. J. Ophthalmol. 1-6, 315258 (2020).
10. L. S. Eppenberger and V. Sturm, “The role of time exposed to outdoor light for myopia prevalence and progression: a literature review,” Clin. Ophthalmol. 14, 1875-1890 (2020).
11. J. Neitz and M. Neitz, “Methods for diagnosing and treating eye-length related disorders,” US patent 8,951,729 B2 (2012).
12. D. I. Flitcroft, E. N. Harb, and C. F. Wildsoet, “The spatial frequency content of urban and indoor environments as a potential risk factor for myopia development,” Inv. Ophthalmol. Vis. Sci. 60, 6452 (2019).
13. A. B. Watson and J. I. Yellott, “A unified formula for light-adapted pupil size,” J. Vision 12(10):12, 1-16 (2012).
14. S. K. Harley and D. H Sliney, “Pupil size in outdoor environments,” Health Physics 115(3), 354-359 (2018).
15. M. D. Witting and D. Goyal, “Normal pupillary size in fluorescent and bright light,” Ann. Emerg.

Med. 41(2), 247-250 (2003).

16. R. A. Gordon and P. B. Donzis, “Refractive development of the human eye,” Arch. Ophthalmol. 103(6), 785-789 (1985).
17. A. Bach, V. M. Villegas, A. S. Gold, W. Shi, and T. G. Murray, “Axial length development in children,” Int. J. Ophthalmol. 12(5), 815-819 (2019).
18. K. S. Mehra, B. B. Khare, and E. Vaithilingam, “Refraction in full-term babies,” Br. J. Ophthalmol. 49, 276-277 (1965).
19. D. L. Ehrlich, O. J. Braddick, J. Atkinson, S. Anker, F. Weeks, T. Hartley, J. Wade, and A. Rudenski, “Infant emmetropization: longitudinal changes in refraction components from nine to twenty months of age,” Optom. Vis. Sci. 74, 822-843 (1997).
20. L. S. Lim, S. Chua, P. T. Tan, S. Cai, Y.-S. Chong, K. Kwek, P. D. Gluckman, M. V. Fortier, C. Ngo, A. Qiu, and S.-M. Saw, “Eye size and shape in newborn children and their relation to axial length and refraction at 3 years,” Ophthalmol. Physiol. Opt. 35(4), 414-423 (2015).
21. D. O. Mutti, G. L. Mitchell, L. A. Jones, N. E. Friedman, S. L. Frane, W. K. Lin, M. L. Moeschberger, and K. Zadnik, “Axial growth and changes in lenticular and cornea power during emmetropization in infants,” Invest. Ophthalmol. Vis. Sci. 46(9), 3074-3080 (2005).
22. H. C. Fledelius, A. S. Christensen, and C. Fledelius, “Juvenile eye growth, when completed? An evaluation based on IOL-Master axial length data, cross-sectional and longitudinal,” Acta. Ophthalmologica 92, 259-264 (2014).
23. A. Carmichael Martins and B. Vohnsen, “Analysing the impact of myopia on the Stiles-Crawford effect of the first kind using a digital micromirror device,” Ophthalm. and Physiol. Opt. 38(3), 273-280 (2018).
24. J. W. L. Tideman, M. C. C. Snabel, M. S. Tedja, G. A. van Rijn, K. T. Wong, R. W. A. M. Kuijpers, J. R. Vingerling, A. Hofman, G. H. S. Buitendijk, J. E. E. Keunen, C. J. F. Boon, A.J. M. Geerards, G. P. M. Luyten, V. J. M. Verhoeven, and C. C. W. Klaver, “Association of axial length with risk of uncorrectable visual impairment for Europeans with myopia,” JAMA Ophthalmol. 134(12), 1355-1363 (2016).
25. J. M. Enoch, “Optical properties of the retinal receptors,” J. Opt. Soc. Am. 53(1), 71-85 (1963).
26. B. Vohnsen, I. Iglesias, and P. Artal, “Guided light and diffraction model of human-eye photoreceptors,” J. Opt. Soc. Am. A 22(11), 2318-2328 (2005).
27. B. Vohnsen, “Directional sensitivity of the retina: A layered scattering model of outer-segment photoreceptor pigments,” Biomed. Opt. Express 5(5), 1569-1587 (2014).
28. B. Chen and W. Makous, “Light capture by human cones,” J. Physiol. 414, 89-109 (1989).
29. F. W. Campbell and D. G. Green, “Optical and retinal factors affecting visual resolution,” J. Physiol. 181(3), 576-593 (1965).

30. D. A. Palmer, “Stiles-Crawford apodization and the Campbell effect,” J. Opt. Soc. Am. A 2(8), 1371-1374 (1985).
31. A. Meadway and L. C. Sincich, “Light propagation and capture in cone photoreceptors,” Biomed. Opt. Express 9, 5543-5565 (2018).
32. W. Li, J. Ball, and S. Chen, “Cone mitochondria act as microlenses to enhance light delivery and confer Stiles-Crawford-like direction sensitivity,” IOVS ARVO abstract 62, 2788 (2021).
33. B. Vohnsen, A. Carmichael, N. Sharmin, S. Qaysi, and D. Valente, “Volumetric integration model of the Stiles-Crawford effect of the first kind and its experimental verification,” J. Vision 17(12), 18:1-11 (2017).
34. J. Neitz and M. Neitz, “Photoreceptor activity patterns and the cause and prevention of myopia,” Optometry and Vision Science 88(3), 424 (2011).
35. S. Gisbert and F. Schaeffel, “M to L cone ratios determine eye sizes and baseline refractions in chickens,” Exp. Eye Res. 172, 104-111 (2018).
36. J. Wallman, M. D. Gottlieb, V. Rajaram, and L. A. Fugate-Wentzek, “Local retinal regions control local eye growth and myopia,” Science 237(4810) 73-77 (1987).
37. W. Shen, M. Vijayan, and J. G. Sivak, “Inducing form-deprivation myopia in fish,” Invest. Ophthalmol. Vis. Sci. 46(5), 1797-1803 (2005).
38. S. A. McFadden and C. Wildsoet, “The effect of optic nerve section on form deprivation myopia in the guinea pig,” J. Comp. Neurol. 528(17), 2874-2887 (2020).
39. H. Liang, D. P. Crewther, S. G. Crewther, and A. M. Barila, “A role for photoreceptor outer segments in the induction of deprivation myopia,” Vision Res. 35(9), 1217-1225 (1995).
40. X. Liu, M. Shen, Y. Yuan, S. Huang, D. Zhu, Q. Ma, X. Ye, and F. Lu, “Macular thickness profiles of intraretinal layers in myopia evaluated by ultrahigh-resolution optical coherence tomography,” Am. J. Ophthalmol. 160(1), 53-61 (2015).
41. S. A. Read, J. A. Fuss, S. J. Vincent, M. J. Collins, and D. Alonso-Caneiro, “Choroidal changes in human myopia: insights from optical coherence tomography imaging,” Clin. Exp. Optom. 102(3), 270-285 (2019).
42. N. Sharmin and B. Vohnsen, “Monocular accommodation response to random defocus changes induced by a tuneable lens,” Vision Res. 165, 45-53 (2019).
43. B. Wang, Q. Zhang, R. Lu, Y. Zhi, and X. Yao, “Functional optical coherence tomography reveals transient phototropic change of photoreceptor outer segments,” Opt. Lett. 39(24) 6923-6926 (2014).
44. W. Gao, B. Cense, Y. Zhang, R. S. Jonnal, and D. T. Miller, “Measuring retinal contributions to the optical Stiles-Crawford effect with optical coherence tomography,” Opt. Express 16(9), 6486-6501 (2008).

45. M. Azimipour, D. Valente, K. V. Vienola, J. S. Werner, R. J. Zawadzki, and R. S. Jonnal, “The optoretinogram: optical measurement of human cone and rod photoreceptor responses to light,” Opt. Lett. 45(17), 4658-4661 (2020).
46. R. M. Hansen and A. B. Fulton, “Development of the cone ERG in infants,” Invest. Ophthalmol. Vis. Sci. 46(9), 3458-3462.
47. J. D. Roarty and J. L. Keltner, “Normal pupil size and anisosocoria in newborn infants,” Arch. Ophthalmol. 108(1), 94-95 (1990).
48. C. Yuodelis and A. Hendrickson, “A qualitative and quantitative analysis of the human fovea during development,” Vision Res. 26(6), 847-855 (1986).
49. L. Vajzovic, A. E. Hendrickson, R. V. O'Connell, L. A. Clark, D. Tran-Viet, D. Possin, S. J. Chiu, S. Farsiu, and C. A. Toth, “Maturation of the human fovea: correlation of spectral-domain optical coherence tomography findings with histology," Am. J. Ophthalmol. 154(5) 779-789 (2012).
50. H. Lee, R. Purohit, A. Patel, E. Papageorgiou, V. Sheth, G. Maconachie, A. Pilat, R. J. McLean, F. A. Proudlock, and I. Gottlob, “In vivo foveal development using optical coherence tomography,” Invest. Ophthalmol. Vis. Sci. 56(8), 4537-4545 (2015).
51. C. A. Curcio, K. R. Sloan, R. E. Kalina, and A. E. Hendrickson, “Human photoreceptor topography,” J. Comp. Neurol. 292(4), 497-523 (1990).
52. M. He, Y. Chen, and Y. Hu, “Prevention of myopia onset,” Ch. 7 in “Updates on myopia,” Editors M. Ang and T. Wong (Springer, Singapore, 2020).
53. L. A. Jones, G. L. Mitchell, D. O. Mutti, J. R. Hayes, M. L. Moeschberger, and K. Zadnik, “Comparison of ocular component growth curves among refractive error groups in children,” Invest. Ophthalmol. Vis. Sci. 46(7), 2317-2327 (2005).
54. C.-Y. Hwang, S. Oh, I.-K. Jeong, and H. Kim, “Stepwise angular spectrum method for curved surface diffraction,” Opt. Express 22(10), 12659-12667 (2014).
55. B. Vohnsen, “Photoreceptor waveguides and effective retinal image quality,” J. Opt. Soc. Am. A 24(3), 597-607 (2007).
56. Lord Rayleigh, “On the dynamic theory of gratings,” Proc. Roy. Soc. A 79, 399-416 (1907).
57. B. Vohnsen, I. Iglesias, and P. Artal, “Directional light scanning laser ophthalmoscope,” J. Opt. Soc. Am. A 22(12), 2606-2612 (2005).
58. D. R. Williams, D. I. A. MacLeod, and M. M. Hayhoe, “Punctate sensitivity of the blue-sensitive mechanism,” Vision Res. 21, 1357-1375 (1981).
59. H. Hofer H, J. Carroll, J. Neitz, M. Neitz, and D. R. Williams, “Organization of the human trichromatic cone mosaic,” J Neurosci. 25(42), 9669–9679 (2005).
60. R. Sabesan, H. Hofer, and A. Roorda, “Characterizing the human cone photoreceptor mosaic via dynamic photopigment densitometry,” PlosOne 10(12) e0144891 (2015).

61. J. K. Bowmaker and H. J. A. Dartnall, “Visual pigments of rods and cones in a human retina,” J. Physiol. 298, 501-511 (1980).
62. R. F. Spaide and C. A. Curcio, “Anatomical correlates to the bands seen in the outer retina by optical coherence tomography: literature review and model,” Retina 31(8), 1609-1619 (2011).
63. A. Hendrickson and D. Drucker, “The development of parafoveal and mid-peripheral human retina,” Behav. Brain Res. 49(1) 21-31 (1992).
64. G. Maden, A. Cakir, D. Icar, B. Erden, S. Bolukbasi, and M. Elcioglu, “The distribution of the photoreceptor outer segment length in a healthy population,” J. Ophthalmol. 4641902 (2017).
65. M. A. Wilk, B. M. Wilk, C. S. Langlo, R. F. Cooper, and J. Carroll, “Evaluating outer segment length as a surrogate measure of peak foveal cone density,” Vision Res. 130, 57-66 (2017).
66. K. Y. Li, P. Tiruveedhula, and A. Roorda, “Intersubject variability of foveal cone photoreceptor density in relation to eye length,” Invest. Ophthalmol. Vis. Sci. 51(12), 6858-6867 (2010).
67. R. P. J. Hughes, S. J. Vincent, S. A. Read, and M. J. Collins, “Higher order aberrations, refractive error development and myopia control: a review,” Clin. Exp. Optometry 103: 68-85 (2020).
68. L. Zheleznyak, A. Barbot, A. Ghosh, and G. Yoon, “Optical and neural anisotropy in peripheral vision,” J. Vision 16(5): 1, 1-11 (2016).
69. A.Jóźwik, M. Asejczyk-Widlicka, P. Kurzynowski, and B. K. Pierscionek, “How a dynamic optical system maintains image quality: Self-adjustment of the human eye,” J. Vision 21(3):6 (2021).
70. B. Swiatczak and F. Schaeffel, “Emmetropic, but not myopic human eyes distinguish positive defocus from calculated blur,” Inv. Ophthalmol. Vis. Sci. 62(3), 14 (2021).
71. A. Fu, F. Stapleton, L. Wei, W. Wang, B. Zhao, K. Watt, N. Ji, and Y. Lyu, “Effect of low-dose atropine on myopia progression, pupil diameter and accommodative amplitude: low-dose atropine and myopia progression,” Br. J. Ophthalmol. 104(11), 1535-1541 (2020).
72. F. Rucker, M. Henriksen, T. Yanase, and C. Taylor, “The role of temporal contrast and blue light in emmetropization,” Vision Res. 151, 78-87 (2018).
73. E. Wells-Gray, S. S. Choi and N. Doble, “The effect of moderate myopia on rod and cone photoreceptor densities in human eyes using AO-SLO imaging,” Inv. Ophthalmol. Vis. Sci. 58, 2994 (2017).
74. C. J. Murphy, K. Zadnik, and M. J. Mannis, “Myopia and refractive error in dogs,” Invest. Ophthalmol. Vis. Sci. 33, 2459-2463 (1992).
75. L. M. Knill, R. D. Eagleton, and E. Harver, “Physical optics of the equine eye,” Am. J. Vet. Res. 38(6), 735-737 (1977).
76. M. Ross, R. Ofri, I. Aizenberg, M. Abu–Siam, O. Pe’er, D. Arad, A. Rosov, E.Gootwine, H. Dvir, H. Honig, A. Obolensky, E.Averbukh, E. Banin, and L. Gantz, “Naturally-occurring myopia and loss of cone function in a sheep model of achromatopsia,” Sci. Rep. 10: 19314 (2020).

77. C. Karouta and R. S. Ashby, “Correlation between light levels and the development of deprivation myopia,” Inv. Ophthalmol. Vis. Sci. 56, 299-309 (2015).
78. E. G. Landis, V. Yang, D. M. Brown, M. T. Pardue, and S. A. Read, “Dim light exposure and myopia in children,” Inv. Ophthalmol. Vis. Sci. 59, 4804-4811 (2018).
79. A. V. Rukmini, M. C. Chew, M. T. Finkelstein, E. Atalay, M. Baskaran, M. E. Nongpiur, J. J. Gooley, T. Aung, D. Milea, and R. P. Najjar, “Effects of low and moderate refractive errors on chromatic pupillometry,” Scientific Reports 9:4945 (2019).
80. N. Bohr, “Light and life,” Nature 131, 457-459 (1933).